

Figure S1

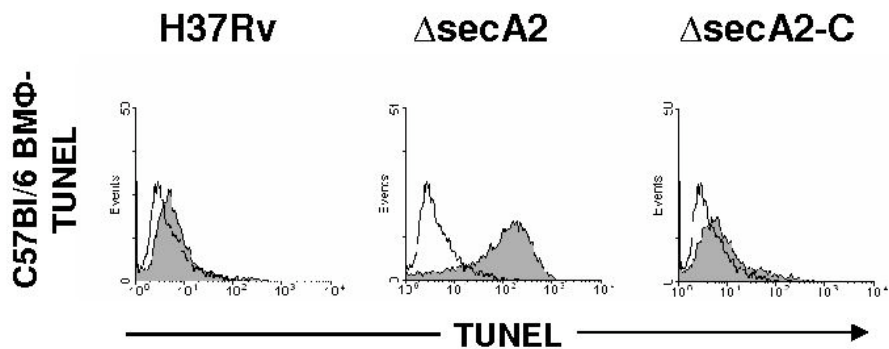
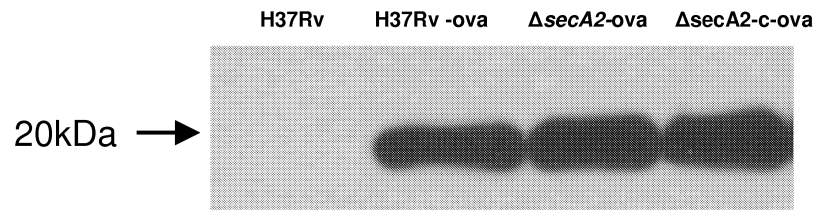
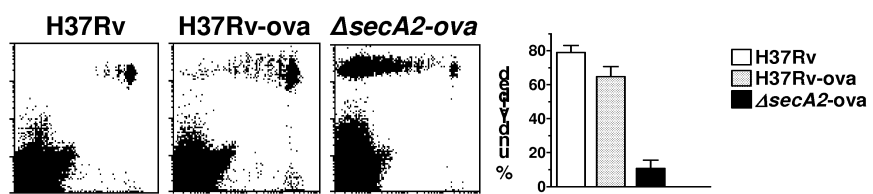


Figure S2

A



B



C

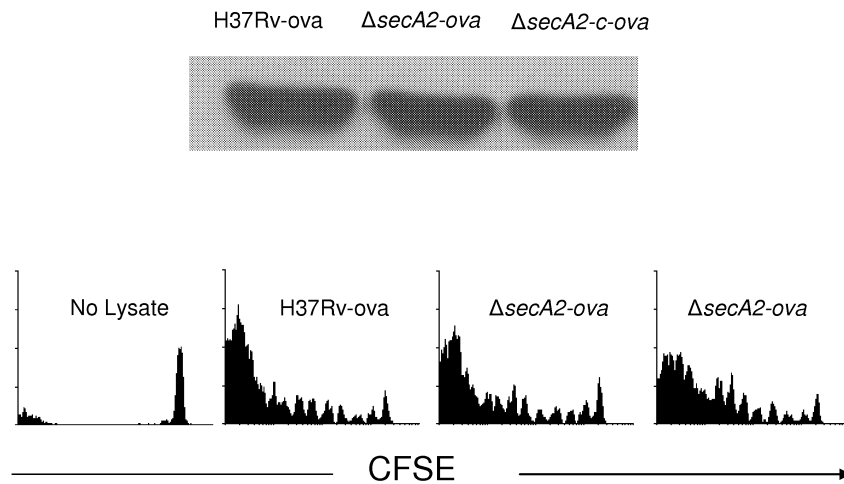


Figure S3

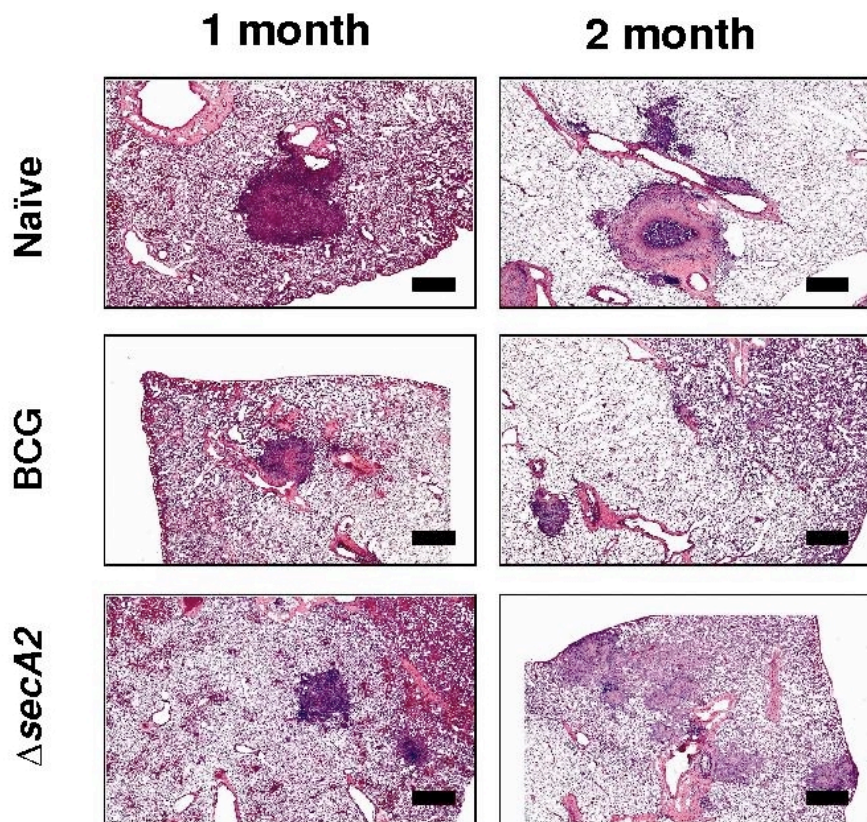
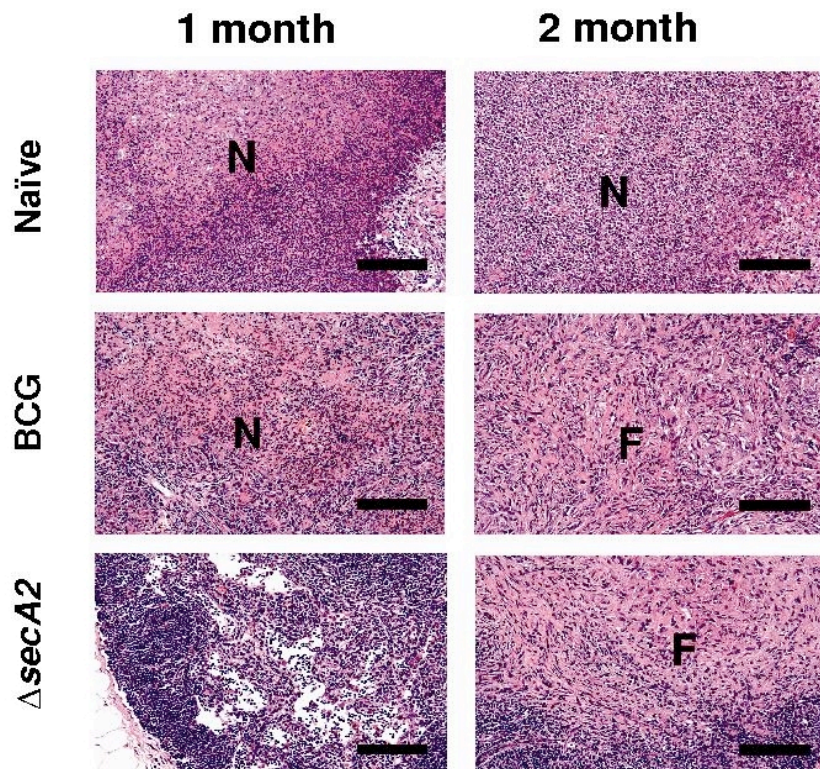


Figure S4



Legends to online supplemental figures

Figure S1. Induction of apoptosis in mouse macrophage by infection with Δ secA2. Bone marrow-derived macrophages from C57BL/6 mice were infected with wild type *M. tuberculosis* (H37Rv), Δ secA2, and Δ secA2-C strains at an MOI of 10 bacilli per macrophage. Cells were stained after 72 hrs with TUNEL reagent, and analyzed by FACS. Representative histograms of TUNEL staining are shown (open histogram, uninfected; grey histogram, infected with H37Rv, Δ secA2 or Δ secA2-C as indicated).

Figure S2. Expression and immunogenicity of ova fusion constructs by recombinant strains of *M. tuberculosis* **A)** Lysates were prepared from cultures of H37Rv, H37Rv-ova, Δ secA2-ova, and Δ secA2-C-ova grown to mid-Log phase and adjusted to an OD₆₀₀ of 1. Equal volumes of adjusted cultures were pelleted and lysed with extraction buffer. Equal amounts of protein (20 μ g) were subjected to SDS-PAGE followed by Western blot analysis using an affinity purified rabbit polyclonal anti-SIINFEKL antibody. **B)** Representative study using adoptive transfer of CFSE-labeled OT-I splenocytes to clearly visualize the transferred population and measure its division and expansion in response to *M. tuberculosis* strains expressing the 19kDa-SIINFEKL fusion protein. Thy1.1⁺ B6.PL mice were injected i.v. with 1x10⁷ CFSE-labeled Thy1.2⁺ splenocytes from OT-I mice, followed one day later by infection with H37Rv, H37Rv-ova, or Δ secA2-ova. CD8⁺ T cell activation and proliferation were assessed by dilution of CFSE in the transferred population at 6 days post infection. Dot plots show

representative mice with gating on B220 negative lymphocytes, and bar graphs show means and standard deviations of the percentages of Thy1.2⁺ cells showing no CFSE dilution (i.e., undivided cells) for two or three mice infected with each of the bacterial strains as indicated. Note that in the experiment shown, a relatively large number of OT-I splenocytes were transferred. Although this leads to an excessively high precursor frequency that causes a partial attenuation of the response, the high cell number transfer has the advantage of allowing the population of undivided CFSE-labeled cells to be clearly visualized.

C) Lysates were prepared from H37Rv-ova, *_secA2*-ova, and *_secA2-C*-ova mid-log phase. Equal volumes of bacterial cultures were boiled for 1 hour followed by sonication. C57BL/6 mice were adoptively transferred with 5×10^5 OT-I splenocytes, followed one day later by subcutaneous injection with lysates containing equivalent amounts of 19kd-SIINFEKL fusion protein (as determined by Western blotting and densitometry) mixed with 20 μ g of the adjuvant QS-21 (Antigenics, New York, NY). Western blots were analyzed on a Kodak image station using Kodak 1D software (Kodak, Rochester, NY). Mice were immunized with 100 μ l of H37Rv-ova lysate, 100 μ l of *_secA2*-ova lysate, or 123 μ l of *_secA2-C*-ova lysate, corresponding to Σ intensity (pixels x arbitrary units of luminescence) values of 136465, 137904, and 111888, respectively. CD8⁺ T cell activation and proliferation were assessed by dilution of CFSE in the transferred population at 5 days post immunization. Cells isolated from draining (inguinal) lymph nodes were stained with antibodies specific to Thy1.2 and B220 plus

SIINFEKL-loaded H-2K^b tetramer. Histograms show tetramer and Thy1.2 positive, B220 negative cells from representative mice.

Figure S3. Low power images of guinea pig lungs. Lungs of unimmunized guinea pigs 1 month and 2 months post-challenge with low dose aerosol of *M. tuberculosis* H37Rv showed early signs of central necrosis (arrow) as well as peribronchial infiltrates of lymphocytes. There was early coagulative necrosis within the center of peribronchial and perivascular granulomas in BCG vaccinated animals. There was no evidence of necrosis in *_secA2* vaccinated animals. Instead, a mixture of infiltrating lymphocytes was observed. At two months post-challenge, extensive coagulative necrosis and dystrophic mineralization was observed for unvaccinated guinea pigs. In BCG vaccinated guinea pigs there was mild resolving inflammation, interlesional fibrosis and neo-vascularization but no evidence of necrosis. In the lungs of *_secA2* vaccinated guinea pigs there was no evidence of necrosis, and coalescing lesions comprised of macrophage and perilesional lymphocytes were observed. Scale bars represent 1 mm.

Figure S4. High power images of guinea pig lymph nodes. The lymph nodes examined were a cluster located at the tracheal bifurcation that consists of the tracheobronchial and cranial mediastinal nodes. At 1 month post-challenge there was extensive coagulative necrosis (N) that accounted for marked lymph node enlargement in naïve animals. The BCG-vaccinated animals had mild

lymph node enlargement due to multiple coalescing foci of granulomatous inflammation with mild lytic necrosis (N). Most notably, the lymph nodes of *_secA2* vaccinated animals were normal with no evidence of inflammation or necrosis.

At two months post-challenge, residual foci of necrosis (N) were evident and early signs of dystrophic mineralization could be seen in unvaccinated animals. BCG vaccinated animals showed signs of replacement of lytic necrosis with extensive fibrous connective tissue (F) leaving virtually no normal tissue. Lymph nodes of *_secA2* vaccinated animals exhibited relatively small foci of mild inflammation with fibrosis (F) but retained normal lymph node parenchyma. Scale bars represent 0.2 mm.